

Utah State University

DigitalCommons@USU

Space Dynamics Laboratory Publications

Space Dynamics Laboratory

1-1-1976

The Sims Technique: An Introduction

Roy W. Esplin
Utah State University

Follow this and additional works at: https://digitalcommons.usu.edu/sdl_pubs

Recommended Citation

Esplin, Roy W., "The Sims Technique: An Introduction" (1976). *Space Dynamics Laboratory Publications*. Paper 42.

https://digitalcommons.usu.edu/sdl_pubs/42

This Article is brought to you for free and open access by the Space Dynamics Laboratory at DigitalCommons@USU. It has been accepted for inclusion in Space Dynamics Laboratory Publications by an authorized administrator of DigitalCommons@USU. For more information, please contact digitalcommons@usu.edu.



THE SIMS TECHNIQUE: AN INTRODUCTION

Roy W. Esplin
Stewart Radiance Laboratory, Utah State University
Bedford, Massachusetts 01730

Abstract

This is a tutorial paper on the SIMS. The SIMS is an acronym for the spectromètre interférentiel à modulation sélective (selective modulation interference spectrometer), recently introduced by Maréchal and Fortunato. The paper reviews the basic principles of operation, the properties, the implementation configurations, and the current investigations of the SIMS at Utah State University. The following properties make the SIMS a powerful spectroscopic instrument. It has an extremely large optical throughput. For example, the SIMS can be configured with a light gathering capability, throughput, thousands of times larger than that of a conventional slit spectrometer. The SIMS does not require a computer to recover the spectrum; it has moderate resolving power, and it has relatively rugged implementation configurations.

Introduction

Spectroscopy instrumentation engineers are consistently being required to design more sensitive spectrometers. To achieve this increased sensitivity, the engineer must often resort to spectrometer configurations which are either complex, delicate, large and bulky, or require extensive data processing to recover the spectrum.

This paper reviews the basic principles of a sensitive yet simple spectrometer which yields the spectrum directly without data processing. The basic principles of this spectrometer were proposed in papers by R. Prat.^(1,2,3) Later Fortunato and Maréchal⁽⁴⁾ developed a spectrometer configuration very similar to Prat's for which they coined the acronym SIMS to describe their spectromètre interférentiel à modulation sélective.

The sensitivity of the SIMS results from its extremely large optical throughput. In fact Fortunato and Maréchal^(4,5) have shown that a SIMS can be constructed with an optical throughput thousands of times larger than that of a conventional grating spectrometer with the same size optics when both spectrometers are operated at the same resolving power. However, it should be realized that the SIMS is not a multiplex spectrometer; it only utilizes energy from one spectral element at a time.

The SIMS utilizes the energy in the selected spectral element by time modulating it while leaving the energy in all the other spectral elements unmodulated. Thus, the SIMS belongs to a class of spectrometers which are referred to as selective modulation spectrometers. These spectrometers scan the spectrum by selectively modulating each spectral element in turn. Selective modulation spectrometers have been constructed using both interferometric and dispersive techniques. For example, the SISAM introduced by P. Connes combines both interferometric and dispersive techniques, while Girard's grill spectrometer is based exclusively on the dispersive technique. The SIMS, on the other hand, is a selective modulation spectrometer based on the interferometric technique.

The SIMS and Girard's grill spectrometer share many properties even though they are interferometric and dispersive respectively. Both spectrometers form transforms of the spectrum along a physical plane with the magnitude of each component function corresponding to the energy of a particular spectral element. Both spectrometers measure the energy in a particular spectral element (recover the magnitude of the component function) by taking the difference between the energy passed through complementary grills placed in the transform plane. However, the transforms formed by the two spectrometers are different; Girard's grill spectrometer forms a convolution type transform⁽⁶⁾ while the SIMS forms a Fourier transform.

Since the SIMS forms a Fourier transform, it also shares some properties with conventional Fourier spectrometers. However, the SIMS forms the Fourier transform in space while conventional Fourier spectrometers form the transform in time. The SIMS uses an electro-mechanical means to invert the transform while a computer is commonly used for this purpose in conventional Fourier spectroscopy. The electro-mechanical inversion method of the SIMS results in simplicity and real time output, but it only utilizes the energy in one spectral element at a time. Theoretically other means could be used to invert the spatial Fourier transform resulting in a spectrometer with the multiplex advantage. The spatial Fourier transform can also be used to make other types of measurements. For example, Fortunato and Maréchal⁽⁷⁾ have proposed several modifications to the SIMS which measure the derivative of the spectrum, the correlation of the spectrum with a reference spectrum, and the correlation of the derivative of the spectrum with the derivative of a reference spectrum.

Principle of Operation

SIMS operation will now be explained by referring to the SIMS schematic drawing shown in

Fig. 1. An optical system depicted as a box in Fig. 1 forms two laterally separated images of the source. The lateral separation distance is represented by the letter T. Thus, a typical point on the source M is imaged as the two points M₁ and M₂. Since M₁ and M₂ are images of the same point, the optical energy radiating from them is coherent and will interfere when superimposed.

It is helpful to first consider the source to be monochromatic with wavelength λ. In this case radiation from the two points M₁ and M₂ forms biased cosine interference fringes along the grill plane. Since at the first peak above the optical center line the optical path difference between radiation from M₁ and M₂ is one wavelength,

$$\lambda = T \sin \theta \approx \frac{Tq}{F} \quad (1)$$

where θ is the angle shown in Fig. 1, F is the focal length of lens L₁, and q is the fringe period. Since the two images formed of each source point are separated by the same distance T, the fringe patterns of all pairs of points coincide in the focal plane of lens L₁ forming high visibility fringes even with an extended source. The high throughput capability of the SIMS results from this ability to form high visibility fringes with an extended source.

A biased cosine transmission grill with the same period as the fringes introduced into the plane of the fringes can be aligned to transmit or block the radiation. If this grill is continuously moved between its transmitting and blocking positions, the radiation passing through the grill will be modulated. This modulated radiation is collected by L₂ onto a detector and the resulting signal is electronically demodulated; the amplitude of this modulated signal corresponds to the source energy. On the other hand if the period of the grill does not match the period of the fringes, the radiation passing through the grill is not modulated. Since modulation depends on the match between the fringe and grill periods, the instrument can be tuned by varying either T or F so that the fringe period for the desired wavelength matches the grill period.

Now consider a polychromatic source. In this case each wavelength will form its own fringe pattern. The superposition of these fringes is the Fourier transform of the source spectrum. For a given F and T only one wavelength will form fringes with the same period as the grill, and if the grill is translated in the fringe plane, only the energy at that wavelength will be modulated. Thus, one spectral element at a time can be selectively modulated, and the entire spectrum can be scanned by varying either T or F.

Resolving Power

As explained previously, modulation occurs when the fringe and grill periods are equal. However, for a practical SIMS there is some modulation when the fringe and grill periods are only approximately equal. It is this unwanted modulation which limits the resolving power of the SIMS. Modulation efficiency is a function of the match between fringe and grill periods. However, in a practical SIMS the grill period is fixed, and the modulation efficiency can be expressed as a function of the fringe period. But since the fringe period is linearly related to the radiation wavelength, modulation efficiency can be expressed as a function of wavelength. Therefore, a plot of modulation efficiency versus wavelength is simply the instrumental profile from which the resolving power can be determined.

In order to obtain a well defined instrumental profile in a practical SIMS, it is necessary to introduce a stop in the fringe plane or its conjugate. For the purpose of the following derivation, a symmetrically located rectangular stop of width W and length L is assumed where L is measured perpendicularly to the fringes. It is also assumed that the grill transmission function is a biased cosine. (Derivations for other grill transmission functions would be similar. A Fourier expansion of the function would first be made, and then the following technique would be applied to each term.)

If q and p are the fringe and grill periods respectively and x₀ is the lateral mask displacement from its symmetrical position, the energy passing through the grill is proportional to

$$e(x_0, q) = W \int_{-L/2}^{L/2} \left[\frac{1}{2} + \frac{1}{2} \cos \frac{2\pi(x-x_0)}{p} \right] \left[\frac{1}{2} + \frac{1}{2} \cos \frac{2\pi x}{q} \right] dx. \quad (2)$$

After expanding Eq. (2) and discarding terms which equal zero,

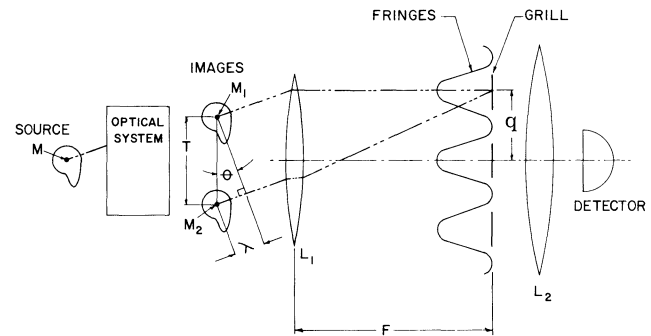


Fig. 1. Schematic SIMS.

$$e(x_o, q) = \frac{W}{4} \left\{ \int_{-L/2}^{L/2} dx + \int_{-L/2}^{L/2} \cos \frac{2\pi x}{q} dx + \cos \frac{2\pi x_o}{p} \int_{-L/2}^{L/2} \left[1 + \cos \frac{2\pi x}{q} \right] \cos \frac{2\pi x}{p} dx \right\}. \quad (3)$$

Since only x_o varies as the grill is moved, the modulation is described by the third term of Eq. (3) which after integration becomes

$$e_M(x_o, q) = \frac{W}{4\pi} \cos \frac{2\pi x_o}{p} \left\{ p \sin \frac{\pi L}{p} + \frac{L}{2} \frac{\sin \pi \left[\frac{1}{q} - \frac{1}{p} \right] L}{\left[\frac{1}{q} - \frac{1}{p} \right] L} + \frac{L}{2} \frac{\sin \pi \left[\frac{1}{q} + \frac{1}{p} \right] L}{\left[\frac{1}{q} + \frac{1}{p} \right] L} \right\}. \quad (4)$$

Since

$$L \approx Np \quad (5)$$

where N is the number of complete grill periods in length L , the worst case ratio of the magnitude of the second term to the first is

$$\frac{L}{2p} \approx \frac{N}{2}. \quad (6)$$

Inasmuch as N is usually 1000 or greater, the first term can be neglected. The third term can also be neglected since physically realizable grills must have positive fringe periods. Substituting Eq. (1) and the definition of wavenumber,

$$\sigma = \frac{\Delta}{\lambda}, \quad (7)$$

in the second term of Eq. (4), the normalized modulation amplitude as a function of wavenumber, the instrumental profile, is given by

$$I(\sigma) = \frac{\sin \pi \left[\frac{\sigma T}{F} - \frac{1}{p} \right] L}{\left[\frac{\sigma T}{F} - \frac{1}{p} \right] L}, \quad (8)$$

and is plotted in Fig. 2. The instrumental profile is a sinc function with the maximum at

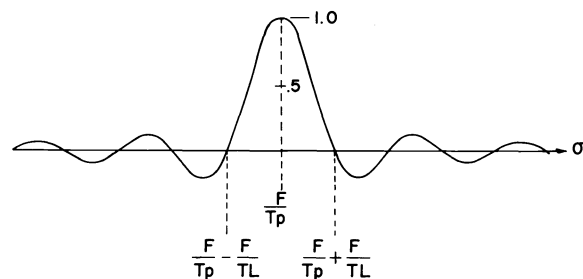
$$\sigma = \frac{F}{Tp}, \quad (9)$$

and the distance from the maximum to the first zero is

$$\Delta\sigma = \frac{F}{TL}. \quad (10)$$

Using Eqs. (5), (9) and (10) the resolving power is

$$R = \frac{\sigma}{\Delta\sigma} \approx N. \quad (11)$$



Thus, the resolving power is simply given by the number of complete grill periods in the stop length. Fig. 2. Instrumental profile for rectangular grill.

As the preceding derivation for a rectangular stop has shown, the instrumental profile depends on the stop's shape. Therefore, the instrumental profile can be slightly modified by using other stop shapes with results analogous to the apodization results of conventional Fourier spectroscopy.

Throughput

The extremely large throughput of the SIMS is its most important characteristic. The throughput of a SIMS depends only on the size and location of its apertures. It does not have the limitation which many spectrometers have that the product of throughput and resolving power equals a constant. The throughput and resolving power of a SIMS can be independently adjusted; for example, the resolving power of a SIMS can be altered simply by using another grill with a different period. Since this does not change either the size or location of any aperture, the throughput is unchanged.

In a well designed SIMS the throughput or étendue is

$$E = \frac{A_S A_F}{Z^2} \tag{12}$$

where A_S is the effective area of either one of the two laterally displaced virtual images of the source as seen from the fringe plane, A_F is the area of the stop in the fringe plane, and Z is the distance between the virtual image and fringe planes. It is necessary to use the effective area since the beams forming the two images are laterally separated, and as a result they may not be limited equally by the apertures of the SIMS. Consequently, since the two beams use different portions of the apertures, a source point may be imaged in one image and not in the other. For example, in the two images shown in Fig. 3, point A is imaged in both as A_1 and A_2 , but points B and C are each only imaged once as the points B_2 and C_1 respectively. Thus, energy from point A contributes to the fringes while that from points B and C does not. If Fig. 3 is examined for points which are imaged in both images, the effective area is the cross hatched area.

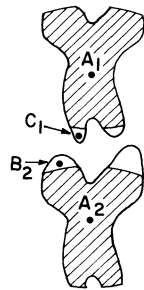


Fig. 3. Unmatched images.

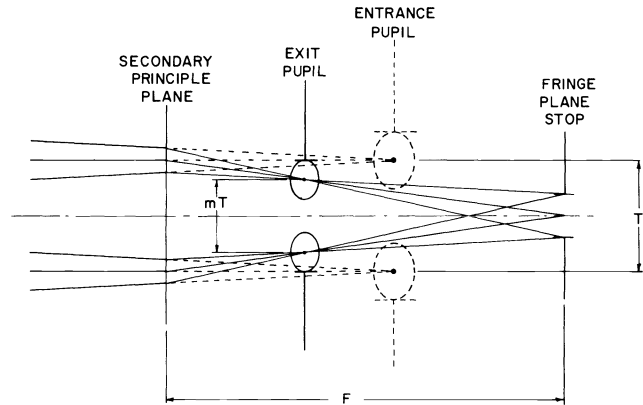


Fig. 4. Design to minimize size of lens L_1 .

Since lens L_1 in Fig. 1 is the only lens requiring significant aberration correction, it is desirable to minimize the size of this lens. The design shown in Fig. 4, which forms the two laterally displaced images in the entrance pupil of L_1 , is an effective method of minimizing the required size of L_1 . This design also results in a sharply defined field of view since the two images are formed within a stop. Notice that in the entrance and exit pupil of L_1 , the lateral separation of the images is T and mT respectively where

$$m = \frac{\text{exit pupil diameter}}{\text{entrance pupil diameter}} \tag{13}$$

If the SIMS is designed so that only the exit pupil of L_1 limits the effective size of the two images, then the effective area is the cross hatched area shown in Fig. 5. The effective image area is given by

$$A_S = \frac{D^2 \pi}{4} - \frac{mT}{2} \sqrt{D^2 - (mT)^2} - \frac{D^2}{2} \sin^{-1} \frac{mT}{D} \tag{14}$$

where D equals the diameter of the exit pupil and

$$T = \frac{F\lambda}{p} \tag{15}$$

Since T is a function of λ , Eqs. (12) and (14) indicate that throughput is a function of λ . If this throughput variation with wavelength cannot be tolerated or if a differently shaped field of view is required, an aperture can be placed at the source (or a conjugate of the source before the lateral shearing occurs). For example, consider a circular aperture at the source such that at the maximum value of T used in the spectral scan, its two images in the exit pupil are as shown in Fig. 6. The effective image area is then circular and given by

$$A_S = \frac{\pi}{4} (D - mT_{\max})^2 \tag{16}$$

where T_{\max} is found by substituting the longest wavelength examined in Eq. (15).

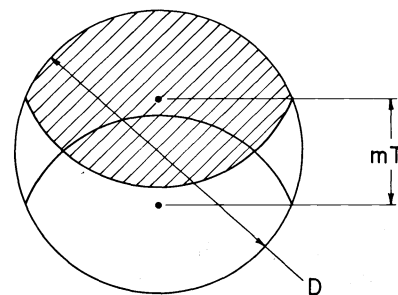


Fig. 5. Effective area completely determined by exit pupil.

An indication of the throughput capability of the SIMS will now be given by computing the throughput of a SIMS with the following practical parameters: W and L equal to 5 cm, Z approximately equal to F which equals 50 cm, D equal to 16 cm, p equal to (1/350) cm, λ_{\max} equal to 2 μm , and m approximately equal to 1. Using these values the resolving power equals 1750, and T_{\max} equals 3.5 cm. If T equal to 3.5 is used in Eqs. (14) and (16), the effective areas are 145.5 cm^2 and 122.7 cm^2 respectively. Substituting these values in Eq. (12), the throughput is 1.46 $\text{cm}^2\text{-sr}$ and 1.23 $\text{cm}^2\text{-sr}$ respectively.

The throughput advantage of the SIMS is clearly demonstrated if the above throughput values are compared with that of a grating monochromator. The throughput of a grating monochromator is

$$E_G \approx \frac{\lambda A_G}{FR} \tag{17}$$

where R is the resolving power, A_G is the projected area of the grating, λ is the slit length, and F is the focal length of the optics forming the slit image. Since the maximum practical (λ/F) ratio is about (1/50), Eq. (17) indicates that the throughput of a grating monochromator with A_G equal to 64 $\pi \text{ cm}^2$ and R equal to 1750 is less than $2.30 \times 10^{-3} \text{ cm}^2\text{-sr}$. Thus, the SIMS throughput values computed above are respectively 635 and 535 times larger than the throughput of a comparable grating monochromator.

Signal-to-Noise Ratio

The effect of noise on SIMS operation depends on whether the noise is photon noise or detector noise.

Since energy from all spectral elements is collected onto the detector even though only one spectral element at a time is demodulated, the energy in all spectral elements contributes photon noise. Therefore, it is advantageous to use an optical passband filter to limit the number of spectral elements striking the detector.

In order to compare the signal-to-noise ratios of a SIMS and a conventional monochromator, it is useful to define the following throughput gain parameter

$$g \triangleq \frac{\text{throughput of SIMS}}{\text{throughput of conventional monochromator}} \tag{18}$$

The value of g may be very large as shown by the SIMS versus grating monochromator comparisons made in the last section.

The signal energy is a factor of g larger for the SIMS than for a conventional monochromator, while the photon noise for a uniform spectrum and a passband filter passing K spectral elements is a factor of \sqrt{Kg} larger for the SIMS than a conventional monochromator. Therefore, when photon noise dominates

$$\frac{(\text{SNR})_{\text{SIMS}}}{(\text{SNR})_{\text{monochromator}}} = \sqrt{\frac{g}{K}} = \sqrt{\frac{g}{K}} \tag{19}$$

where SNR indicates the signal-to-noise ratio. Thus, for photon noise limited conditions with a uniform spectrum, if the throughput gain is larger than the number of spectral elements in the optical filter passband, then the signal-to-noise ratio will be larger for the SIMS than the monochromator. If the spectrum is not uniform but consists of only a few lines, the signal-to-noise advantage of the SIMS at these line peaks will be larger than that given by Eq. (19).

The advantage of the SIMS is much greater when the dominant source of noise is detector noise. In this case the noise will be the same for both the SIMS and the monochromator if the same detector system is used for both spectrometers. Therefore, when the detector noise is the dominant source of noise

$$\frac{(\text{SNR})_{\text{SIMS}}}{(\text{SNR})_{\text{monochromator}}} = g \tag{20}$$

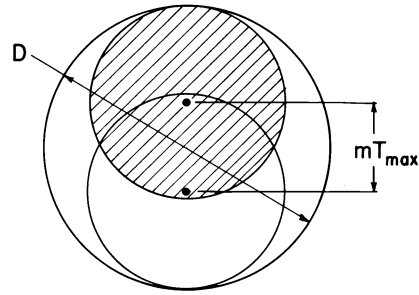


Fig. 6. Effective area with circular stop at source.

Practical ImplementationImage Doubling

Practical designs for forming the two separated images can be classified as cyclic, birefringent and other. One possible cyclic design is shown in Fig. 7. This design, which is based on the Sagnac interferometer, was used by Fortunato and Maréchal in their first SIMS paper.⁽⁴⁾ For this design,

$$T = 2e \quad (21)$$

where e , as shown in Fig. 7, is the distance the scanning mirror is translated from its symmetrical position. If Eq. (21) is substituted in Eq. (15) and the resulting relation solved for λ , the wavelength of the spectral element modulated is

$$\lambda = \frac{2pe}{F} \quad (22)$$

It follows from Eq. (22) that

$$\Delta\lambda = \left[\frac{2p}{F} \right] \Delta e \quad (23)$$

where Δe is the required translation of the scanning mirror to change the wavelength of the modulated energy an amount equal to $\Delta\lambda$. Thus, a linear mirror motion results in a linear wavelength scan. If the required wavelength change is equal to $\delta\lambda$ where $\delta\lambda$ is defined by

$$R = \frac{\lambda}{\delta\lambda} \quad (24)$$

then using Eqs. (5), (11), (23) and (24) the required mirror motion is

$$\delta e = \frac{F\lambda}{2pN} = \frac{F\lambda}{2L} \quad (25)$$

Eq. (25) indicates that the required mirror motion to scan one spectral element is linearly related to the wavelength. Since for a practical SIMS the ratio F/L is on the order of ten, δe is on the order of five times the wavelength.

Since for small angles the change in separation distance is linearly related to the angular change of either mirror, small spectral scans can be made by rotating a mirror. The effects of mirror rotation are directly proportional to the size of the Sagnac; that is, the larger the s dimension in Fig. 7 the larger the wavelength scan for a given angular rotation. Thus, a rapidly scanning SIMS could be constructed by using a piezoelectric crystal to rotate one of the mirrors.

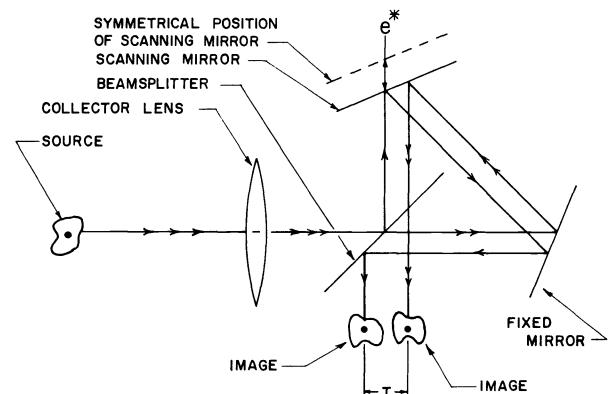
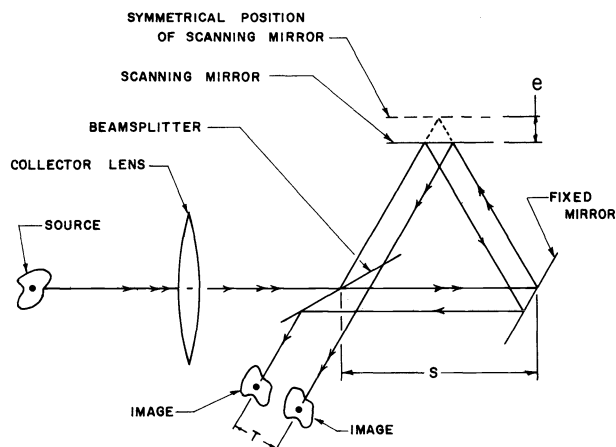


Fig. 7. Cyclic design for image doubling. Fig. 8. Improved cyclic design for image doubling.

Another cyclic design which is a modification of the Sagnac is shown in Fig. 8. Since the angles between the optical beams and the beamsplitter normal are sixty and forty-five degrees respectively for Figs. 7 and 8, the configuration of Fig. 8 uses the beamsplitter more efficiently. In addition, the ninety degree separation between entering and exiting beams of Fig. 8 is more convenient for mounting optics than the sixty degree separation of Fig. 7. For the configuration of Fig. 8

$$T = \sqrt{2} e^* \quad (26)$$

where e^* , as shown in Fig. 8, is the distance the scanning mirror is translated from its symmetrical position. The wavelength of the modulated spectral element is

$$\lambda = \frac{\sqrt{2} p e^*}{F} , \tag{27}$$

and

$$\Delta\lambda = \left[\frac{\sqrt{2} p}{F} \right] \Delta e^* . \tag{28}$$

Since both cyclic designs use the same components to form both images, they are relatively rugged, and spectral scanning requires motion of only one component. Since half the energy is directed back toward the source, the transmission of both these cyclic designs is less than fifty percent. Finally, if the beamsplitting surface is mounted on a substrate, a compensator of the same thickness must be used.

Maréchal and Fortunato⁽⁸⁾ have used the birefringent configuration shown in Fig. 9. In this configuration wavelength scanning is done by varying the separation distance between the birefringent prisms, and the fringes are made to move across a stationary grill by rotating the analyzer. Since in this configuration the shearing is done in the solid birefringent prisms, this configuration is particularly rugged. In order to maximize throughput, it is the author's belief that the birefringent prisms should be field widened Wollaston prisms.⁽⁹⁾

Other optical designs which are not cyclic or birefringent can also be used to form the two images; for example, the configurations shown in Figs. 10 and 11 were used by Prat⁽²⁾ and Sabater⁽¹⁰⁾ respectively. These configurations have the disadvantage that two components must be adjusted to change the separation distance T . However, these configurations can be useful to get very large values of T .

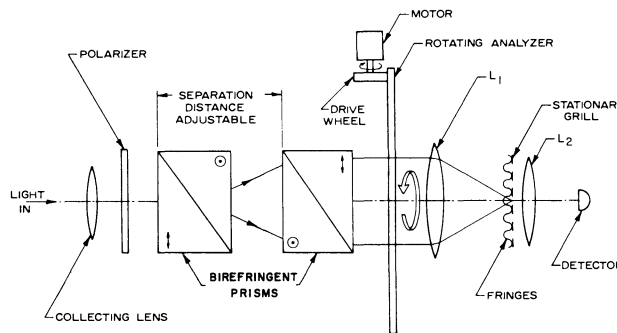


Fig. 9. SIMS based on polarization.

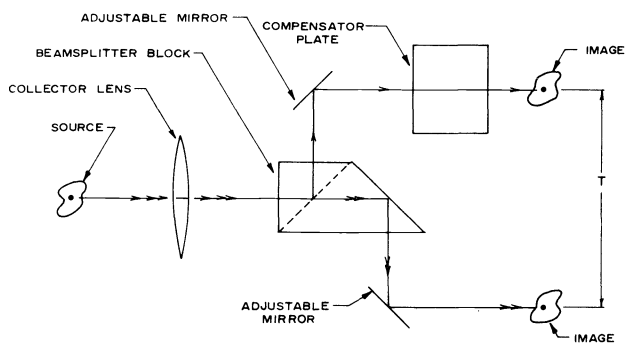


Fig. 10. A noncyclic image doubling design.

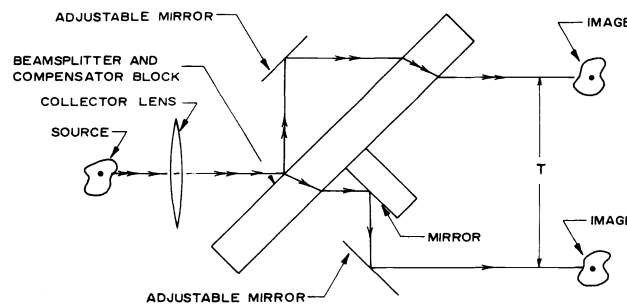


Fig. 11. Another noncyclic image doubling design.

Optical Quality

The optical quality of the collecting lens shown in Figs. 7 through 11 is not critical since the beam is sheared after passing through this component. The condenser lens shown in Fig. 1 need not be highly corrected either because its only function is to collect the radiation onto the detector.

Since the remaining optical components determine the path differences upon which the fringe formation depends, the quality of these optical components is more critical. In order to form high visibility fringes the fringe patterns from all points on the source must coincide. Since this means that the lens L_1 in Fig. 1 must superimpose all rays emitted at the same angle, this lens must be corrected for a source at infinity. Its blur spot width must be significantly less than the grill period. However, since the fringes lie approximately along straight lines, its blur spot length may be significantly longer than the grill period. Thus, spherical aberration and coma are the most serious aberrations in L_1 . The quality of the optical components which shear the optical beam before it enters L_1 must be such that the path difference error which they introduce is less than $\lambda/2$.

Formation of high visibility fringes is the basic requirement, but the shape of the

fringes is also important. A practical lens can be corrected to form a small blur spot, but it will still have some residual distortion. This distortion causes the fringes to be curved rather than straight, and it also causes a gradual change in the fringe period across the field. The residual distortion is commonly neutralized by using a photograph of the monochromatic fringe pattern as a grill.

Since photography is limited to the visible and near infrared spectral regions, new methods of producing grills to match the fringe shape need to be developed. Three possible methods are suggested. First, develop a reflective SIMS configuration. Since such a configuration would have no chromatic aberrations, a grill could be photographed using visible light for use in the infrared spectral region. Second, design the SIMS to have the same shape fringes at one particular visible wavelength as it does in the infrared spectral region. Then a grill photographed at that visible wavelength could be used in the infrared region. Third, use the optical prescriptions of the components in a computer program which computes the fringe shape. Then a computer generated grill could be used.

Relative Motion Between Fringes and Grill

If the optical design produces high visibility fringes and the grill matches the shape of the fringes, modulation is introduced by time varying the lateral displacement x_o between the grill and the fringes. Eq. (4) indicates that the resulting normalized time varying electrical signal is

$$v = \cos \frac{2\pi x_o}{p} \tag{29}$$

Thus, v goes from a maximum to a minimum if x_o varies from 0 to $p/2$. Since Eq. (29) is periodic, variations in x_o much larger than $p/2$ will also produce modulation. However, it is advantageous to use small variations in x_o since this assures that the match between grill and fringe shape is maintained, and also because it is mechanically easier to accurately control the grill motion. Eq. (29) indicates that x_o should be a triangular function of time. However, a physical object can be moved much more rapidly in a sinusoidal fashion. If

$$x_o(t) = \frac{p}{4} (1 - \cos \omega t) \tag{30}$$

is substituted in Eq. (29), then

$$v = 2J_1\left(\frac{\pi}{2}\right) \cos \omega t - 2J_3\left(\frac{\pi}{2}\right) \cos 3 \omega t + \dots \tag{31}$$

where $J_1, J_3, \dots J_k$ are Bessel's functions of the first kind of order k . Since $J_1\left(\frac{\pi}{2}\right)$ is approximately equal to .567,

$$v \approx 1.13 \cos \omega t \tag{32}$$

if the higher harmonies are eliminated by electronic filtering.

The requirement for relative motion between fringes and grill can be eliminated with the configuration shown in Fig. 12. This method, which is similar to the statistical method used with Girard's grill spectrometer, was suggested by Fortunato and Maréchal.⁽⁷⁾ If one grill is located with x_o equal to zero and the other grill with x_o equal to $p/2$, then Eq. (29) indicates that the difference between the two signals is the required measurement. Since this configuration eliminates the need for mechanical motion to produce modulation, it should prove useful for measuring rapidly varying sources.

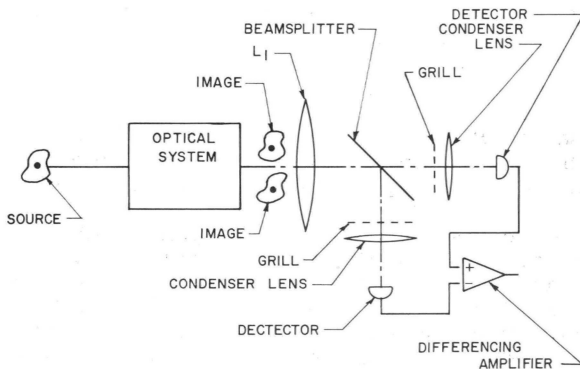


Fig. 12. Configuration not requiring fringe or grill motion.

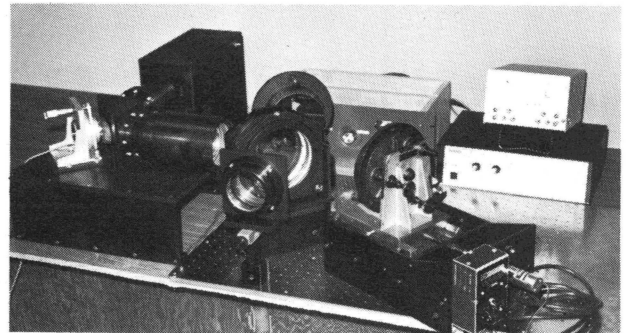


Fig. 13. Utah State University's prototype.

Utah State University's Prototype

SIMS experimentation is currently being conducted by the author with the laboratory prototype shown in Fig. 13 which is configured using the cyclic configuration of Fig. 8. A five element lens is used to form the fringes. The lens elements are mounted in two cells at right angles with a piezoelectrically rotated plane mirror which translates the fringes across a stationary grill mounted between them. The lens has a focal length of 412 mm and an entrance aperture of 78 mm. Its half angle field of view is 2.6 degrees. Its wavefront aberration is on the order of $\lambda/4$ from .6328 to 1.2 μm .

Acknowledgements

The author gratefully acknowledges Dr. George Vanasse, of AFGL, who brought the SIMS to the author's attention and who has made many insightful suggestions.

The research reported in this paper was funded by the Defense Nuclear Agency under Sub-task L25AAXHX632 and by the Air Force Geophysics Laboratory under Contract F19628-72-C-0245.

References

1. Prat, R., "Nouvelle méthode spectrométrique interférentielle," Japanese Journal of Applied Physics, Vol. 4, pp. 448-450. 1965.
2. Prat, R., "Spectrométrie et spectrographie interférentielles par dédoublement achromatique transversal de la source. I," Optica Acta., Vol. 18, pp. 213-244. 1972.
3. Prat, R., "Spectrométrie et spectrographie interférentielles par dédoublement achromatique transversal de la source. II," Optica Acta., Vol. 18, pp. 247-268. 1972.
4. Fortunato, G., and A. Maréchal, "Spectromètre interférentiel à modulation sélective," Comptes rendus., Vol. 274, Series B, pp. 931-934. 1972.
5. Maréchal, A., and G. Fortunato, "Recent Developments in Selective Modulation Spectrometry," Proceedings of the Ninth International Congress of the International Commission for Optics, pp. 739-749. 1974.
6. Mertz, L., Transformations in Optics, John Wiley & Sons, Inc. 1965.
7. Fortunato, G., and A. Maréchal, "Possibilités de dérivation et de corrélation de spectres dans les spectromètres interférentiels à grille," Comptes rendus., Vol. 276, Series B, pp. 527-530. 1973.
8. Maréchal, A., "New Perspectives in Interferometric Spectrometry," Presented at the 1975 Annual Meeting of the Optical Society of America.
9. Francon, M., Optical Interferometry, Academic Press. 1966.
10. Sabater, J., Private communication. Dec. 1973.

Question: (Alan B. Dauger, McDonnell Douglas) Is the throughput advantage of the SIMS instrument over the grating instrument still obtained if we have the advantage of using a collimated beam source and a collecting telescope with the grating instrument?

Answer: The formula presented here is still correct and applies to the basic grating instrument whose throughput cannot be improved upon.